International Journal of Robotics and Automation (IJRA)
Vol. 6, No. 4, December 2017, pp. 252~268
ISSN: 2089-4856, DOI: 10.11591/ijra.v6i4.pp252-268

Identifying the Optimal Controller Strategy for DC Motors

M. R. Qader
Departement of Electrical and Electronics Engineering P.O. Box 32038 University of Bahrain, Kingdom of Bahrain

Article Info

Article history:

Received Jun 23, 2017
Revised Sep 10, 2017
Accepted Sep 24, 2017

Keyword:

Controller strategy
DC motor
LQR
PI
PID

ABSTRACT

The aim of this study is to design a control strategy for the angular rate (speed) of a DC motor by varying the terminal voltage. This paper describes various designs for the control of direct current (DC) motors. We derive a transfer function for the system and connect it to a controller as feedback, taking the applied voltage as the system input and the angular velocity as the output. Different strategies combining proportional, integral, and derivative controllers along with phase lag compensators and lead integral compensators are investigated alongside the linear quadratic regulator. For each controller transfer function, the step response, root locus, and bode plot are analysed to ascertain the behaviour of the system, and the results are compared to identify the optimal strategy. It is found that the linear quadratic controller provides the best overall performance in terms of steady-state error, response time, and system stability. The purpose of the study that took place was to design the most appropriate controller for the steadiness of DC motors. Throughout this study, analytical means like tuning methods, loop control, and stability criteria were adopted. The reason for this was to suffice the preconditions and obligations. Furthermore, for the sake of verifying the legitimacy of the controller results, modelling by MATLAB and Simulink was practiced on every controller.

Corresponding Author:

M. R. Qader,
Departement of Electrical and Electronics Engineering,
P.O. Box 32038 University of Bahrain, Kingdom of Bahrain.
Email: mredi@uob.edu.bh

1. INTRODUCTION

Direct current (DC) motors are an important component in many electrical devices, converting electrical power to mechanical motion. They work by supplying a current through a conductor within a magnetic field; the current is forced by the torque and produces motion. DC motors are ubiquitous, with almost all industries and households using them in various equipment or appliances. These applications require the speed of the motor to be controlled to drive processes such as the arm of a robot. The control can be either manual or automatic. Many studies have investigated the optimal control of DC motors to achieve the desired results. In this study, we compare several control strategies to evaluate their accuracy and stability.

The aim of this study is to design a control strategy for the angular rate (speed) of a DC motor by varying the terminal voltage. This is done by setting the desired angular velocity to unity and examining the best design criteria achieved by different control strategies.The number of techniques and studies reported over recent years shows the importance of this topic. Here, after presenting a definition of control, we provide an overview of the history of DC motor controlling techniques, and review some of the methods used to implement the work described in this paper.

DC motor controllers are an example of controlling devices. They might include a manual or automatic means of starting and stopping the motor, selecting forward or reverse rotation, regulating the speed, limiting the torque, and protecting against overloads and faults [1].Controlling the motor speed is not a new idea, and is fundamental in the design of feedback control systems. This is done by receiving an input signal from a measured process variable, comparing this value with that of a predetermined control point value (set point), and determining the appropriate output signal required by the final control element to provide corrective action within a control loop. Previous studies and designs have not focused on the real benefit, but have instead applied only slight increments to the control parameters.

Modern controllers use power electronics and microprocessors, and are of varying complexity. The choice of controller often depends on the control objectives and controller cost. DC motor controllers must be able to handle unknown load characteristics and parameter variations. Proportional-integral-derivative (PID) controllers are most commonly used to control DC motors. These offer several important features and are easy to implement. The disadvantage of PID controllers is that they often overshoot the desired objective value following sudden changes in load torque. Additionally, PID controller parameters are very difficult to control, making it hard to achieve the optimal state. To overcome this disadvantage, control methods such as linear quadratic regulators (LQRs) have been developed [2,13]. LQRs offer robustness in terms of minimizing a given cost function [3].

The simplicity, reliability, and minimal cost of DC motors means that they are often preferred over other motors [4]. The best strategy for controlling the speed of a DC motor is to use a PID controller and LQR, which provides better transient parameters [5]. The robustness of LQR ensures an accurate dynamic response [6]. In addition, LQR displays better high-range flexibility and control when compared with other controllers [7,13]. Therefore, LQR is suitable for robotics applications and process control, because it improves system stability, effective control, and balancing properties [8].

2. DESIGN AND IMPLEMENTATION

2.1 Mathematical model of a DC motor

A simplified mathematical model of a DC motor can be used to build the motor transfer function. The schematic diagram of a DC motor in Figure 1 shows the electrical circuit of the armature and the free body diagram of the rotor. From this, the mathematical model can be built [1]. The transfer function is derived from the DC motor equations, which are divided into a mechanical part, electrical part, and the interconnection between them. The equation for the electrical part can be derived as shown in equations (1) and (2):

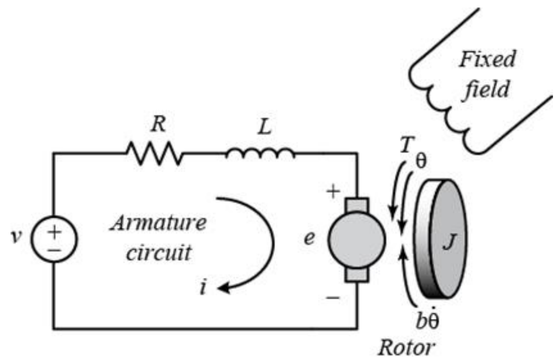

Figure 1. DC motor schematic diagram

$$V(s) = Ra\,Ia + S\,La\,Ia + KØ\,w \tag{1}$$

$$Ia(s) = \frac{V - KØ\,w}{Ra + S\,La} \tag{2}$$

where $Ea = KØ\,w$
V : motor terminal voltage (V)
W : motor speed (rad/s)
Ia : winding current (A)
KØ: back electromotive force (EMF) constant (Vs/rad)
Ra : terminal resistance (Ω)
La : terminal inductance (H)

The equation for the mechanical part can be derived using Newton's law, which states that the summation of electrical and load torques is equal to the load and motor inertia multiplied by the derivative of the angular rate as shown in equations (3-6).

$$\mathrm{J}\frac{\mathrm{dw}}{\mathrm{dt}} = \mathrm{Te} - \mathrm{TL} \tag{3}$$

$$\mathrm{J}\frac{\mathrm{dw}}{\mathrm{dt}} = \mathrm{K}\emptyset\ \mathrm{Ia} - \mathrm{TL} - \mathrm{bw} \tag{4}$$

$$Jsw = \mathrm{K}\emptyset\ \mathrm{Ia} - \mathrm{TL(s)} - \mathrm{bw} \tag{5}$$

$$\mathrm{W(s)} = \frac{\mathrm{K}\emptyset\ \mathrm{Ia} - \mathrm{TL}}{(\mathrm{Js} + \mathrm{b})} \tag{6}$$

where: J: load and motor inertia (kg×m2)
b: damping friction (N×m×s/rad)
TL: load torque (N×m)
Te: electrical torque (N×m)

As the voltage is the input to the system and the speed is the output, the required transfer function is symbolized by w(s)/v(s). This form is derived by dividing equation (8) by equation (3). It can also be found by drawing the block diagram of a DC motor using the same equations as shown in Figure 2.

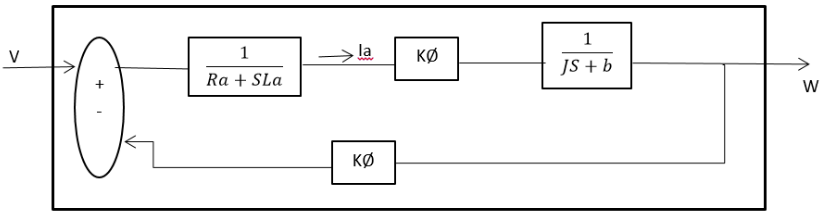

Figure 2. Block diagram of a DC motor

The diagram illustrates a closed loop and Root locus analysis for DC motor system as shown in Figure 3. Therefore, it is possible to use the root locus analysis equation (7):

$$\frac{C}{R} = \frac{G}{1+GH} \tag{7}$$

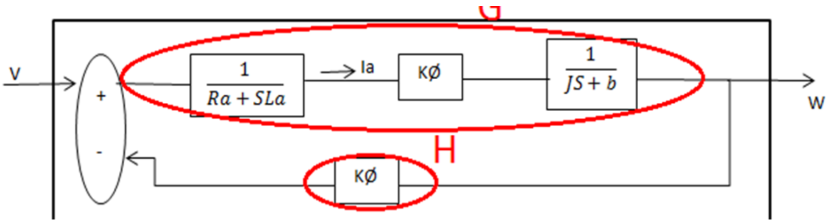

Figure 3. Root locus analysis for DC motor system

From Figure 3 and equation (7), the transfer function for a DC motor can be derived as shown in equations (8) and (9):

$$\frac{w(s)}{V(s)} = \frac{\left(\frac{\mathrm{K}\emptyset}{Ra+SLa}\right)\left(\frac{1}{JS+b}\right)}{1 + \mathrm{K}\emptyset\left(\frac{\mathrm{K}\emptyset}{Ra+SLa}\right)\left(\frac{1}{JS+b}\right)} \tag{8}$$

Or

$$\frac{w(s)}{V(s)} = \frac{K\text{Ø}}{(K\text{Ø})^2 + (Ra+SLa)(JS+b)} \quad (9)$$

2.2 Dynamic system of a DC motor

From Figure 1, assuming a constant excitation field armature, the voltage can be reformed as shown in equations (10-16):

$$V = Ra\,Ia + La\frac{d\,Ia}{dt} + K\text{Ø}\,w \quad (10)$$

$$d\frac{Ia}{dt} = -\frac{Ra}{La}ia - \frac{K\varphi}{La}w + \frac{1}{La}V \quad (11)$$

Using Newton's second law:

$$J\frac{dw}{dt} = Te - TL - bw \quad (12)$$

where b is the damping friction. Thus,

$$\frac{dw}{dt} = \frac{1}{J}(K\varphi\, Ia - TL - bw) \quad (13)$$

$$s = -\frac{Ra}{La}\,Ia\,(s) - \frac{K\varphi}{La}w(s) + \frac{1}{La}V(s) \quad (14)$$

$$\left(s + \frac{Ra}{La}\right)Ia(s) = -\frac{K\varphi}{La}w(s) + \frac{1}{La}V(s) \quad (15)$$

$$\left(s + \frac{b}{J}\right)w(s) = \frac{1}{J}K\varphi\,Ia(s) - \frac{1}{J}TL(s) \quad (16)$$

To use a dynamic system method, we should specify the states, input, and output of the system. In a DC motor system, the current (I) and angular rate (dW/dt) are the states, the applied voltage (V) is the input, and the angular velocity (w) is the output. As the system is linear as shown in equations (17-22), the state space can be written in the form:

$$\dot{x}\,(t) = [A]\,x(t) + [B]\,u(t) \quad (17)$$

$$\dot{y}(t) = [C]\,x(t) + [D]\,u(t) \quad (18)$$

where: $x^{\cdot}$ (t) denotes the state vectors i and w
$y^{\cdot}$ (t) is the output w
u (t) is the input V

$$\dot{x}\,(t) = \frac{dx(t)}{dt} = \frac{d}{dt}\,(i \text{ and } w) \quad (19)$$

[A] = state matrix (n×n)
[B] = input matrix (n×p)
[C] = output matrix (q×n)
[D] = feed forward (zero) matrix (q×p)
Following the method above, and from equations (11) and (13), the state space becomes:

$$\frac{d}{dt}\begin{bmatrix} i \\ w \end{bmatrix} = \begin{bmatrix} -\frac{Ra}{La} & -\frac{K\varphi}{La} \\ \frac{k\varphi}{J} & -\frac{b}{J} \end{bmatrix}\begin{bmatrix} i \\ w \end{bmatrix} + \begin{bmatrix} \frac{1}{la} \\ 0 \end{bmatrix}V \quad (20)$$

$$W=[0\ 1]\begin{bmatrix} i \\ w \end{bmatrix} + [0]V \quad (21)$$

$$A=\begin{bmatrix} -\frac{Ra}{La} & -\frac{K\varphi}{La} \\ \frac{k\varphi}{J} & -\frac{b}{J} \end{bmatrix},\ B=\begin{bmatrix} \frac{1}{la} \\ 0 \end{bmatrix},\ C=[0\ 1],\ D=[0] \quad (22)$$

Therefore, the block diagram for the dynamic system of a DC motor can be illustrated as shown in Figure 4.

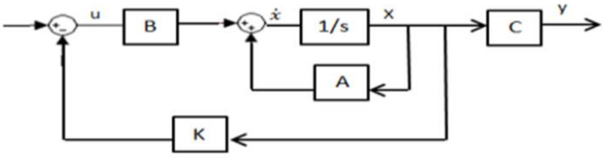

Figure 4. Dynamic system block diagram

2.3 Open loop of DC motor angular velocity

To obtain a transient response in the situations studied in this paper (i.e. the open loop condition), we use a simple DC motor model with the parameters listed in Table 1.

Table 1. Parameters of DC Motor

Parameter	Symbol	Value	Unit
Motor terminal voltage	V	input	Volt (V)
Motor speed	w	output	rad/s
Back EMF constant	KØ	0.01	V s/rad
Terminal resistance	Ra	2	Ohms Ω
Terminal inductance	La	0.5	Henrys (H)
Load and motor inertia	J	0.02	kg m^2
Damping friction	b	0.2	N m s/rad

After substituting these parameter values into the variables in equation (9), the transfer function of the DC motor open loop becomes as shown in equation (23):

$$\frac{w(s)}{V(s)} = \frac{0.01}{0.01\, s\hat{}2 + 0.14\, s + 0.4001} = \frac{1}{(s+9.998)\,(s+4.002)} \tag{23}$$

Figure 5 shows the open loop step response of angular velocity (wss = 0.025 rad/s, ts = 1.2 s) has a large steady-state error (0.975 rad/s).

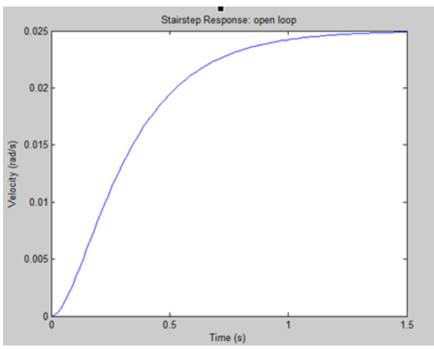

Figure 5. Open loop step response of DC motor angular velocity

Even using the dynamic system method, the open loop can be tested by computing the eigenvalues of matrix A, which represent the poles of the system:

Poles = -4.0017 and -9.9983

From the above result, there are no poles in the right half-plane, which means that the system is unstable in the open loop condition.

2.4 Closed loop of DC motor angular velocity

As the open loop step response has a very large steady-state error and the system is unstable, the closed loop will be designed with different controller strategies to eliminate the error and enhance the system transient response. Figure 6 shows a system with unity feedback and a feed-forward compensator (C) in series with the DC motor for added controllability.

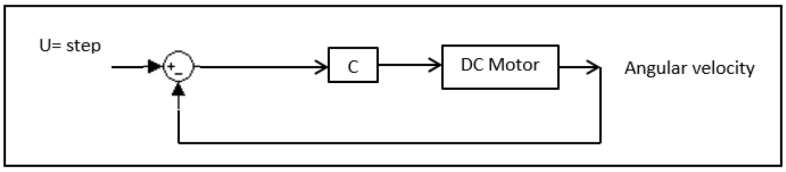

Figure 6. Closed loop of DC motor

2.5 Controlling DC motor angular velocity through different compensation techniques

The main objective of this paper is to design a feed-forward compensator that will drive the DC motor angular velocity to unity. Different control strategies will be applied and compared in terms of the steady-state error in the step response, settling time, and stability.

There are three main controllers: proportional controller, integral controller, and derivative controller. This paper also examines the LQR controller and three types of compensator: phase lag compensator, lead integral compensator, and lead lag compensator.

2.5.1 Proportional controller design

Known as the P-only controller, this type operates directly according to the error signal. Mathematically, this relationship can be interpreted as shown in equation (24):

$$Pout = K1 \times e(t) \tag{24}$$

Where K1 is the proportional gain. Figure 7 shows a block diagram when using the P-only controller.

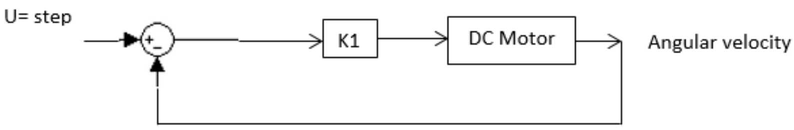

Figure 7. P-only controller block diagram

2.5.2 Integral controller design

Also known as the actuating signal, this controller is directly proportional to the integral of the error signal. The corresponding equation (25) is:

$$Pout = K2 \times \int_0^t e\,(t) \tag{25}$$

Where K2 is the integral controller gain. The block diagram for this controller is shown in Figure 8.

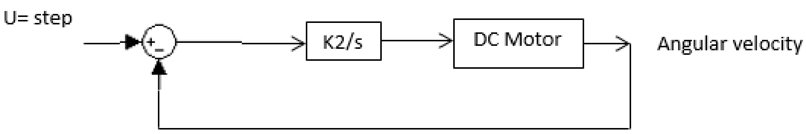

Figure 8. Integral controller block diagram

2.5.3 Derivative controller design

Sometimes called the rate controller, this is the mathematical opposite of the integral controller, being directly proportional to the derivative of the error signal. Thus, its equation (26) is:

$$Pout = K3 \times \frac{de(t)}{dt} \tag{26}$$

Where K3 is the derivative controller gain. The block diagram of this controller is shown in Figure 9.

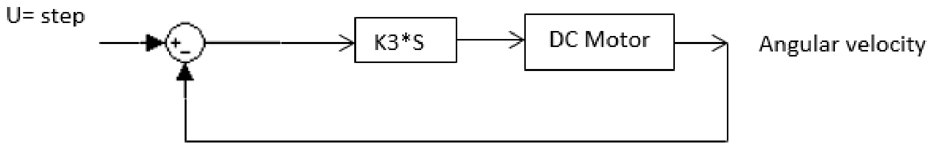

Figure 9. Derivative controller block diagram

Using these three main controllers, the following strategies can be derived:

a. Proportional-Integral Controller
b. Proportional-Integral-Derivative Controller
c. Phase lag compensator
d. Lead integral compensator
e. Lead lag compensator

2.5.4 Proportional-integral (PI) controller design

PI control is widely used in industry to handle subtle variations in conditions. As the name suggests, this is a combination of the proportional and integral controllers, and has the equation (27):

$$Pout = K1 \times e(t) + \ K2 \times \int_0^t e\ (t) \tag{27}$$

Where K1 and K2 are the proportional gain and integral gain, respectively. The block diagram of a PI controller is shown in Figure 10.

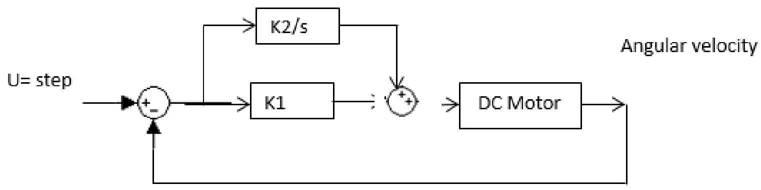

Figure 10. PI controller block diagram

2.5.5 Proportional-integral-derivative controller design

The PID controller is a control loop feedback mechanism that is widely used in industrial control systems [9, 12]. PID control combines the proportional, integral, and derivative controllers to correct the error between the output and the desired input or set point. The general equation for a PID controller has the form equation (28):

$$Pout = K1 \times e(t) + \ K2 \times \int_0^t e\ (t) + K3 \times \frac{de(t)}{dt} \tag{28}$$

Figure 11 shows the block diagram for a PID controller.

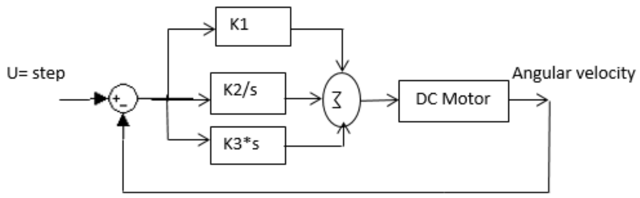

Figure 11. PID controller block diagram

2.5.6 Phase lag compensator design

A system consisting of some gain, one negative zero, and one negative dominating pole close to the origin is known as a lag network. A lag compensator adds this network to the control system. Generally, the lag compensator has the form [10, 11] equations (29-33):

$$C = K\,\frac{1}{\alpha}\,\frac{s+z}{s+P} \tag{29}$$

or

$$C = K\,\frac{1}{\alpha}\,\frac{\frac{s}{Z}+1}{\frac{s}{P}+1} \tag{30}$$

where $Z(the\ zero) < 0$

$$P(the\ pole) < 0$$

$$Z > P \tag{31}$$

$$\alpha = \frac{Z}{P} > 1 \tag{32}$$

$$T = \frac{1}{Z} = \frac{1}{\alpha P} \tag{33}$$

Substituting these terms into equation (30), the general form of the lag compensator becomes equations (34-35):

$$C = K\,\frac{Ts+1}{\alpha Ts+1} \tag{34}$$

Or

$$C = \frac{Kc}{\alpha}\,\frac{s+1/T}{s+1/\alpha T} \tag{35}$$

The zero and the pole are selected to be close to each other to the left of the origin; a large value of α gives better results. The general form above is multiplied directly to the control system, as shown in Figure 12.

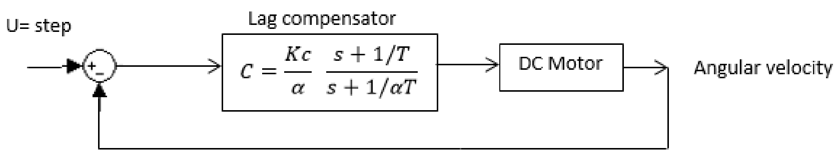

Figure 12. Phase lag compensator block diagram

2.5.7 Lead integral compensator design

In the lead network, the system zero is closer to the origin than the pole. The general form for this compensator [3] as shown in equation (36):

$$C = Kc \ \frac{s+1/T}{s+1/\alpha T} \tag{36}$$

The compensator is directly connected to the control system as shown in Figure 13.

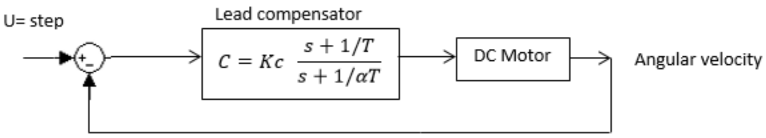

Figure 13. Lead integral compensator block diagram

2.5.8 Lead lag compensator design

The lead lag compensator is combines the lead and lag compensators in the control system, as shown in Figure 14. The general equation for the lead lag compensator as shown in equation (37):

$$c = Kc \left(\frac{s+\frac{1}{Tlead}}{s+\frac{1}{\alpha Tlead}}\right)\left(\frac{s+\frac{1}{Tlag}}{s+\frac{1}{\alpha Tlag}}\right) \tag{37}$$

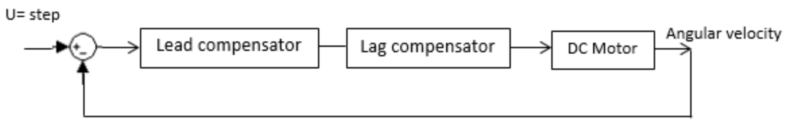

Figure 14. Lead lag compensator block diagram

2.5.9 LQR controller design

State feedback using LQR follows equations (17) and (18). Figure 15 shows the LQR state feedback configuration. This design is classified as the optimal control system. However, this will realize practical components that provide the designed operating performance. Therefore, the performance indices can be readily adjusted in the time domain. As a result, the steady state and the transient performance indices are specified in the time domain.

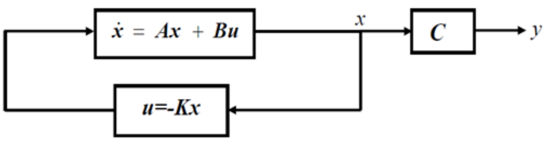

Figure 15. LQR structure

The performance of a control system can be represented by integral performance measures. Therefore, the design of the system must be based on minimizing some performance index, such as the integral of the squared error. The specific form of the performance index [11] as shown in equations (38-39):

$$j = \int_0^{tf} [(tracking\ error\ )^2 + (weighted\ inputs)^2\ ]dt \tag{38}$$

or

$$J = \int_0^{tf=\infty} (x^T\, Qx + u^T Ru)dt \tag{39}$$

where x denotes the state vector, x^T is the transpose of x, tf is the final time, and R, Q denote weighting factors and controller design parameters, respectively, which are selected by trial and error. The control input u is given by equation (40):

$$u = -Kx = [K1\ K2\ K3 \ldots Kn]x \tag{40}$$

From the state space of the system as shown in equation (41):

$$\dot{x} = A\,x + B\,u = Hx \tag{41}$$

where H is known. Its maximum value is given by equations (42-45):

$$H = x^T Qx + u^T Ru + \lambda^T\,(Ax + Bu) \tag{42}$$

$$\dot{x} = A\,x + B\,u = \left(\frac{\partial H}{\partial \lambda}\right)^T \tag{43}$$

$$-\dot{\lambda} = \left(\frac{\partial H}{\partial x}\right)^T = Qx + A^T\,\lambda \tag{44}$$

$$0 = \frac{\partial H}{\partial u} = -Ru + \lambda^T\,B \tag{45}$$

Therefore equation (46),

$$u = -R^{-1}\,B^T\,\lambda \tag{46}$$

Because equation (47)

$$\lambda(t) = P(t)\,x(t) \text{ or } \lambda = P\,x \tag{47}$$

we have that equations (48-53)

$$u = -R^{-1}\,B^T\,Px \tag{48}$$

$$\dot{\lambda} = \dot{P}x + P\dot{x} \tag{49}$$

$$\dot{\lambda} = \dot{P}x + P(A\,x - BR^{-1}\,B^T\,Px) \tag{50}$$

$$-\dot{P}x - PA\,x + PBR^{-1}\,B^T\,Px = Qx + A^T\,Px \tag{51}$$

$$-\dot{P} = PA + A^T\,P - PBR^{-1}\,B^T\,P + Q \tag{52}$$

$$0 = PA + A^T\,P - PBR^{-1}\,B^T\,P + Q \tag{53}$$

The block diagram of the DC motor under LQR control is shown in Figure 16.

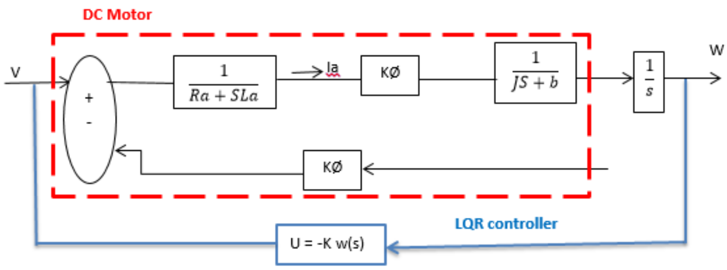

Figure 16. Block diagram of the DC motor with LQR control

3. RESULTS AND ANALYSIS

The controller designs in the previous section were implemented in a DC motor module to test their capabilities. This section presents the results in detail.

3.1 Proportional controller

The proportional controller is a simple strategy. It works as an amplifier to the input signal and is inversely proportional to the steady-state error. Thus, when the gain of the compensator increases, the steady-state error should decrease. Two proportional controllers were tested. The first has a proportional gain equal to one, which means the input signal is not amplified. This is identical to the closed loop condition, and so the transfer function of the system as shown in equation (54):

$$\frac{w(s)}{V(s)} = \frac{0.01}{0.01\ s\text{^}2 + 0.14\ s + 0.4101} = \frac{1}{(s+9.827)\ (s+4.173)} \qquad (54)$$

Figure 17 shows the closed loop step response of the DC motor angular velocity (wss = 0.0244 rad/s), where the steady-state error is no less than its value in the open loop condition (0.9756 rad/s). The settling time is 1.1 s.

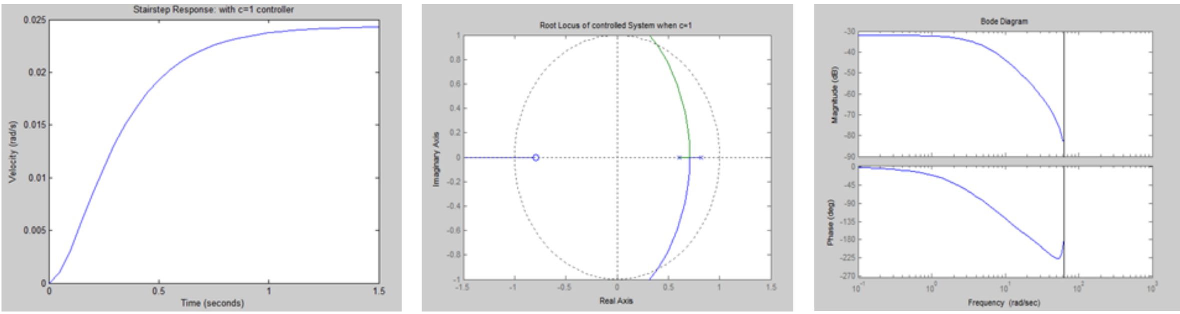

Figure 17. Step response, root locus, and Bode plot of closed loop DC motor system angular velocity

In the second proportional controller, the gain was set to 100. The transfer function of the system becomes equation (55):

$$\frac{w(s)}{V(s)} = \frac{1}{0.01\ s\text{^}2 + 0.14\ s + 1.4} \qquad (55)$$

Figure 18 shows the step response of the DC motor angular velocity (wss = 0.8427 rad/s, ts = 0.75 s). The steady-state error is lower (0.1573 rad/s), but has not been eliminated. The system is unstable because there are poles in the right half of the S-plane and the system overshoots the steady state, but it will become stable as the proportional gain is increased.

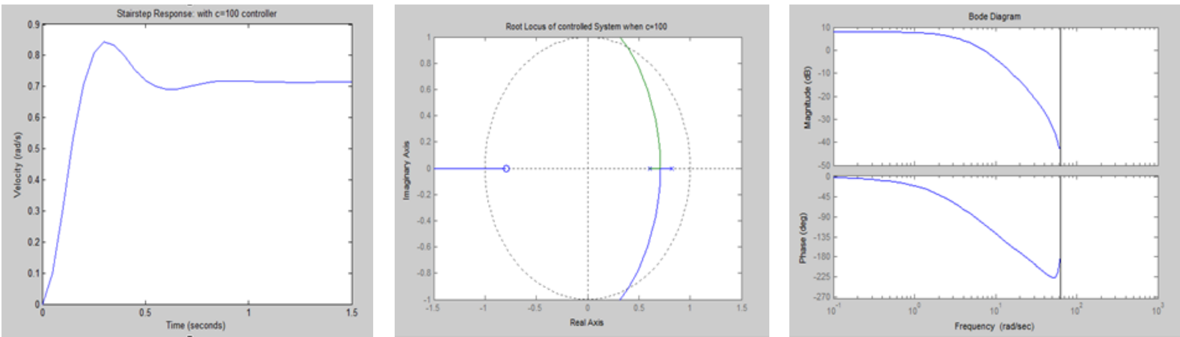

Figure 18. Step response, root locus, and Bode plot of DC motor system angular velocity when C = 100

In conclusion, if the proportional gain is equal to unity, the system will remain unchanged. However, if the gain value is greater than unity, the error signal will be amplified and the steady-state error will decrease, making the system more stable. Unfortunately, using this controller may lead to an increase in the overshoot.

3.2 Integral controller

The integral controller reduces the error by multiplying the transfer function of the system by K/s, where K is the gain (constant) and s is the Laplace transform. The step response, root locus, and Bode plot of DC motor system angular velocity using an integral controller as shown in Figure 19. The gain value is 100, so the transfer function of the system becomes as shown in equation (56):

$$\frac{w(s)}{V(s)} = \frac{1}{0.01\,s^3 + 0.14\,s^2 + 0.4001\,s + 1} \tag{56}$$

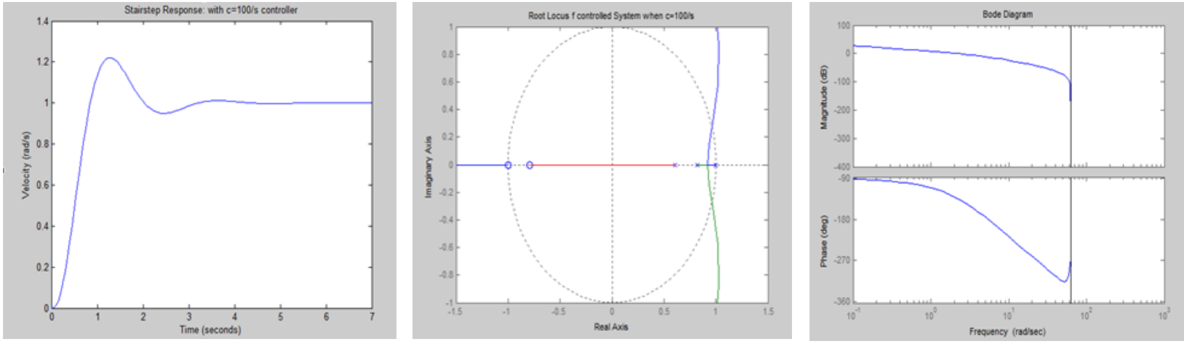

Figure 19. Step response, root locus, and Bode plot of DC motor system angular velocity using an integral controller

From Figure 19, it is clear that the integral controller can fully eliminate the steady-state error (wss = 1.2202 rad/s). However, it also has the disadvantage of producing a closed loop system with a slower response time (tss = 2.95 s), large overshoot value (22.0151), and the potential for system instability as the gain increases. It can be concluded that the benefit of this type of controller is its ability to reduce the error to zero. However, stability is not guaranteed, as the system may oscillate randomly. This controller also has a slower response time.

3.3 Proportional-integral controller

In the PI controller described by equation (27), K1 and K2 were each set to 100. Thus, the equation becomes equation (57):

$$c = 100 * (1 + s)/s \tag{57}$$

Therefore, the transfer function of this system as shown in equation (58):

$$\frac{w(s)}{V(s)} = \frac{100\,(s+1)}{(s+0.7703)\,(s^2 + 13.23s + 129.8)} \tag{58}$$

Figure 20 shows that the PI controller eliminates the steady-state error (wss = 0.9998 rad/s). The system remains stable as the controller gain increases, and the overshoot is reduced to zero, but the system settling time is still large (tss = 3.25 s).

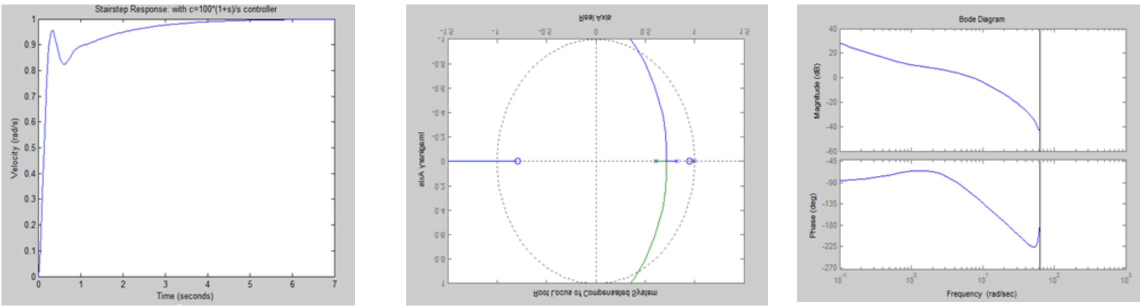

Figure 20. Step response, root locus, and Bode plot of DC motor system angular velocity using a PI controller

3.4 Derivative controller

This type the system applies feed-forward control equal to the derivative of the error. Thus, the transfer function of the system as shown in equation (59):

$$\frac{w(s)}{V(s)} = \frac{0.01\ s}{0.01\ s\verb|^|2 + 0.15\ s + 0.4001} \tag{59}$$

From Figure 21, the derivative controller drives the motor speed to zero, so the steady-state error will be unacceptable. In addition, the noise signal produced in the system is amplified, so the derivative controller cannot be used alone. However, this type of controller has the advantage of an improved transient response. Hence, there is no need to use a derivative controller if the control objective has a slow response, but it could be beneficial if the control objective responds quickly.

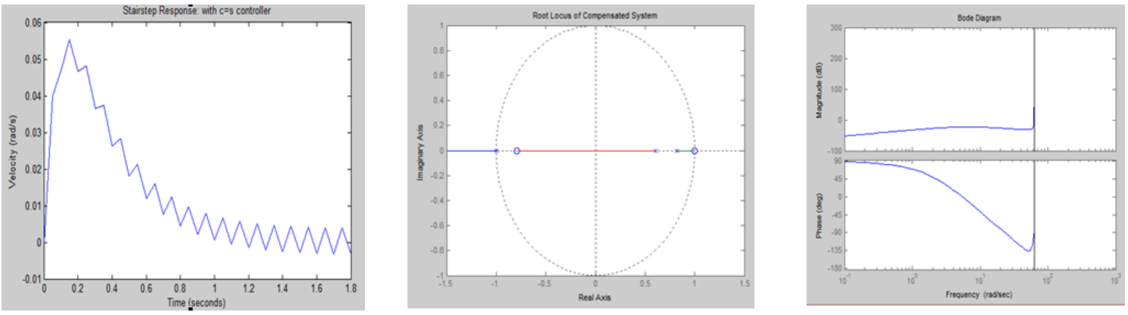

Figure 21. Step response, root locus, and Bode plot of DC motor system angular velocity using a derivative controller

3.5 Proportional-integral-derivative controller:

Transferring equation (28) from the time domain to the S-domain, we obtain as shown in equation (60):

$$\mathrm{c} = \mathrm{k1} + \frac{\mathrm{k2}}{\mathrm{s}} + \mathrm{k3} * \mathrm{s} \tag{60}$$

Setting k1, k2, and k3 equal to 100, the overall closed loop transfer function becomes equation (61):

$$\frac{w(s)}{V(s)} = \frac{s\verb|^|2 + s + 1}{0.01\ s\verb|^|3 + 1.14\ s\verb|^|2 + 1.4\ s + 1} \tag{61}$$

From Figure 22, we see that the PID controller eliminates the steady-state error (wss = 1.0122 rad/s), but the settling time remains large (tss = 3.4355 s). The root locus plot indicates that the system will have poles on the imaginary axis as the gain increases.

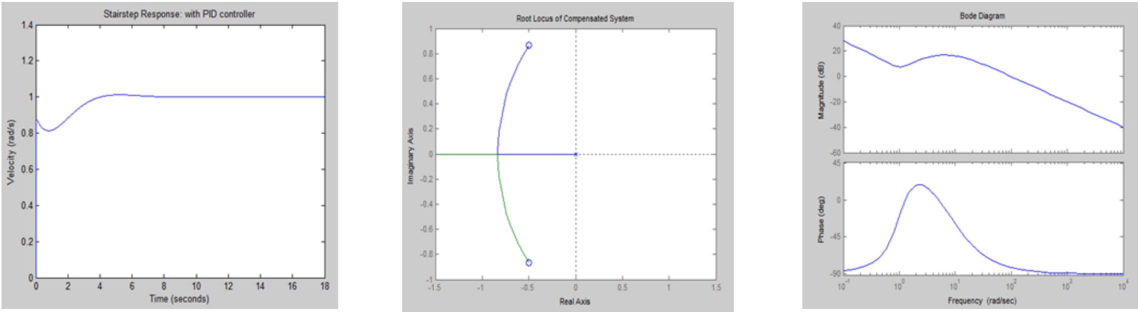

Figure 22. Step response, root locus, and Bode plot of DC motor system angular velocity using a PID controller

3.6 Phase lag compensator

Setting kc, α, and T to 1000, 10, and 10, respectively, in equation (35), the feed-forward phase lag compensator controlling the motor can be written as shown in equation (62):

$$c = 100 * \frac{s+0.1}{s+0.01} \tag{62}$$

Therefore, the transfer function of the system will be equation (63):

$$\frac{w(s)}{V(s)} = \frac{100(s+0.1)}{(s+0.07476)\ (s\text{^}2 + 13.94s + 139.1)} \tag{63}$$

From Figure 23, we can see that the steady-state error is practically eliminated (wss = 0.9611rad/s, ess = 0.0385). This technique produces a slow response (settling time is very large, tss = 34 s) and large rise time. The system is not subject to instability as the gain increases.

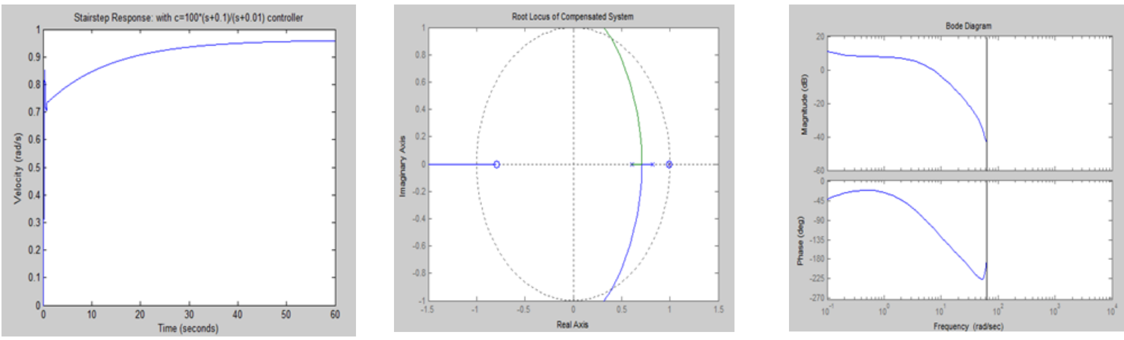

Figure 23. Step response, root locus, and Bode plot of DC motor system angular velocity using a phase lag compensator

3.7 Lead integral compensator

This controller combines the integral compensator to reduce the steady-state error with the lead compensator to improve the settling time. To achieve this, we multiply equation (36) by 1/s to give equation (64):

$$c = Kc * \frac{s+\frac{1}{T}}{s\left(s+\frac{1}{\propto T}\right)} \tag{64}$$

Setting Kc, α, and T to 100, 10, and 10, respectively, we have equation (65):

$$c = 100 * \frac{s+10}{s(s+100)} \tag{65}$$

Therefore, the transfer function of the system becomes equation (66):

$$\frac{w(s)}{V(s)} = \frac{\text{s + 10}}{\text{0.01 s^4 + 1.14 s^3 + 14.4 s^2 + 41.01 s + 10}} \tag{66}$$

From Figure 24, it can be noted that the lead integral compensator eliminates the steady state error (wss = 0.9999 rad/s), but has a large settling time (tss = 14.75 s) and results in an unstable system as the gain increases. Thus, using this technique gives a slow response, but will improve the steady-state error.

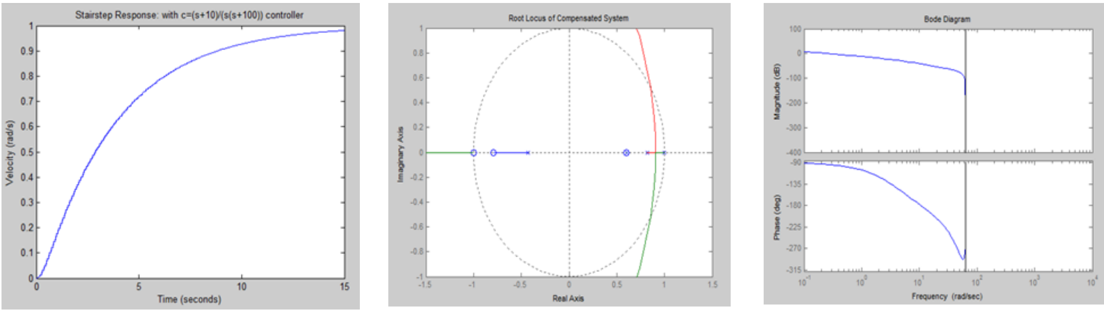

Figure 24. Step response, root locus, and Bode plot of DC motor system angular velocity using a lead integral compensator

3.8 Lead lag compensator

The lead compensator provides a fast response but results in an unstable system, whereas the lag compensator gives a stable system with a slow response time. Therefore, using a lead lag compensator may be more accurate.

The system is controlled by a compensator equation (67) equal to:

$$c = \frac{100(s+10)(s+0.1)}{(s+100)(s+0.01)} \tag{67}$$

Therefore, the transfer function of the system becomes equation (68):

$$\frac{w(s)}{V(s)} = \frac{\text{s^2 + 10.1 s + 1}}{\text{0.01 s^4 + 1.14 s^3 + 15.41 s^2 + 50.25 s + 1.4}} \tag{68}$$

Figure 25 shows that the steady-state error is eliminated (wss = 0.7136 rad/s), but the settling time is very large (tss = 127.65 s). The system is not subject to instability as the gain increases.

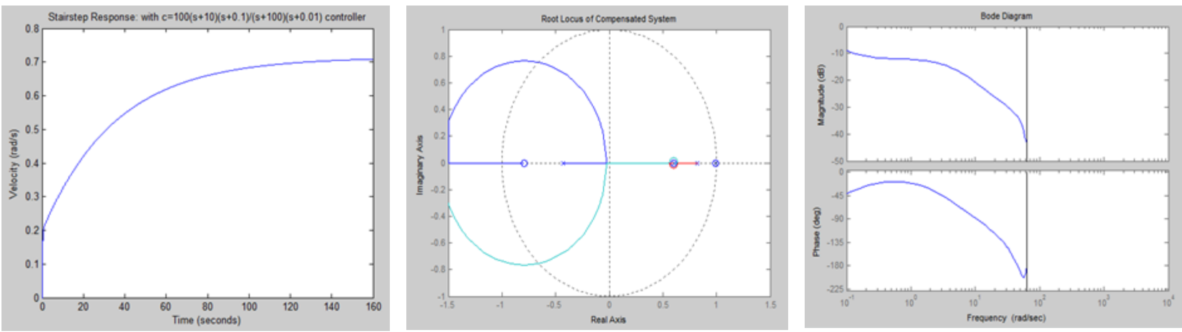

Figure 25. Step response, root locus, and Bode plot of DC motor system angular velocity using a lead lag compensator

3.9 Linear quadratic regulator

The LQR function is used to determine the state feedback control gain as k = 41.0100 and to find the transfer function of the system. This gives in equations (69) and (70):

$$\frac{w(s)}{V(s)} = \frac{44.72}{s^3 + 15.05\, s^2 + 55.2\, s + 44.72} \tag{69}$$

or

$$\frac{w(s)}{V(s)} = \frac{44.7214}{(s+9.95)\,(s+3.961)\,(s+1.135)} \tag{70}$$

Figure 26 shows the step response, root locus, and Bode plot of the DC motor system using an LQR controller. In the steady state, the error has been fully eliminated (wss = 1 rad/s), and the settling time is small (tss = 1.0488 ≈ 1 s). There is no overshoot and the system is completely stable.

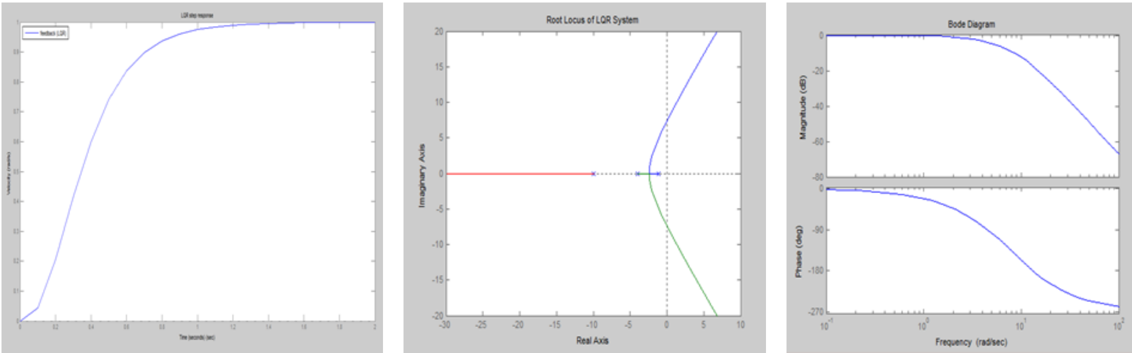

Figure 26. Step response, root locus, and Bode plot of DC motor system angular velocity using an LQR controller

3.10 Comparison between all strategies

The results from all strategies are presented in Table 2, and the step responses of all controllers considered in this study are shown in Figure 27. From these results, it is clear that the LQR controller is the most stable, as the rise time and settling time are very small and the steady-state error is zero. The phase lag controller exhibits good stability, but suffers from a high rise time and settling time.

Table 2. Comparison among all strategies

Controller	Velocity	Steady-state error	Settling time	Rise time	Overshoot	Stability
Proportional c=1	0.0244	0.9756 (large)	1.1	0.6	0	unstable
Proportional c=100	0.8427	0.2858 (quite large)	0.75	0.15	17.9888	unstable
Integral	1.2202	1.5987e-014≈0 (eliminated)	2.95	0.55	22.0151	unstable
Proportional Integral	0.9998	6.1062e-015≈0 (eliminated)	3.25	0.25	0	unstable
Derivative	0	Not acceptable	-	-	-	unstable
Proportional Integral Derivative	1.0122	0 (fully eliminated)	3.4355	2.2122	1.2232	unstable
Phase Lag	0.9611	0.0385≈0 (eliminated)	34	12.4000	0	stable
Lead Integral	0.9999	7.8160e-014≈0 (eliminated)	14.75	8.1	0	unstable
Lead Lag	0.7136	0.2858 (quite large)	127.65	70.3	0	Unstable
Linear quadratic regulator	1	0 (fully eliminated)	1.0488	0.5617	0	stable

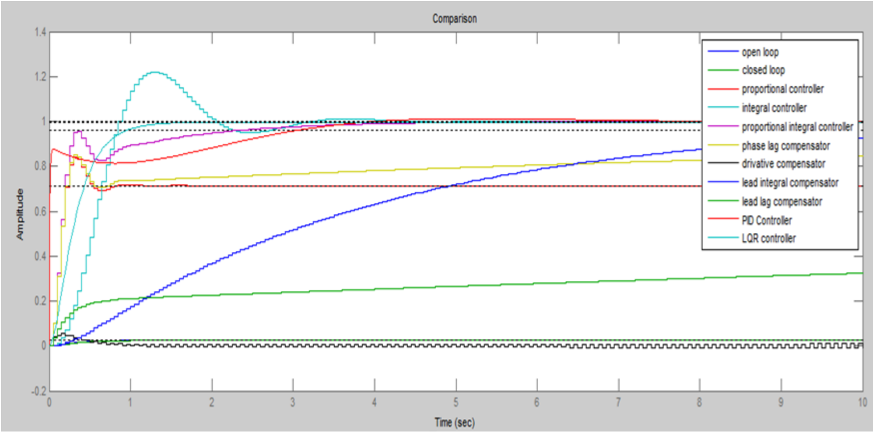

Figure 27. Comparison among all strategies used to control step response of DC motor system angular velocity

4. CONCLUSION

Many applications require the speed of a DC motor to be accurately controlled. Therefore, a control system for a DC motor was designed with the objective of controlling the angular speed to be unity with the best steady state and transient performance. Several types of controllers were applied to the problem, and the results given by the different controller strategies were compared.

Based on the step response, root locus, and Bode plot results for each controller considered in this study, it is clear that the LQR controller achieves the best steady state and transient response performance. This controller can fully eliminate the steady-state error with a very small transient settling time. There is no overshoot and the system is completely stable.

REFERENCES

[1] Monk S., (2012), Programming Arduino Getting Started with Sketches, 1st Edition, McGraw Hill.
[2] Ahmed A. H. O., "*Optimal Speed Control for Direct Current Motor Using Linear Quadratic Regulator*", Journal of Science and Technology – Engineering and Computer Sciences, Vol. 14, No. 2, Dec. 2013.
[3] Chengaiah Ch. and Venkateswarlu K., "*Comparative Study On Dc Motor Speed Control Using Various Controllers*", International Journal of Advanced Research in Electrical, Electronics, and Instrumentation Engineering, Vol. 3, Issue 1, Jan. 2014.
[4] Ma Y., Liu Y. and Wang Elissa C., "*Design of Parameters Self-tuning Fuzzy PID Control for DC Motor*", in Proceedings of Second International Conference on Industrial Mechatronics and Automation (ICIMA), Vol. 2, pp. 345–348, 2010.
[5] Dwivedi R. and Dohare D., "*PID Conventional Controller and LQR Optimal Controller for Speed Analysis of DC Motor: A Comparative Study*", International Research Journal of Engineering and Technology, Vol. 2, Issue 8, Nov. 2015.
[6] Shrivastval V. and Singh R., "*Performance Analysis of Speed Control of Direct Current (DC) Motor using Traditional Tuning Controller*", International Journal of Emerging Technology and Advanced Engineering, Vol. 4, Issue 5, May 2014.
[7] Al-Mulla Hummadi R. M. K., "*Simulation of Optimal Speed Control for a DC Motor Using Linear Quadratic Regulator (LQR)*", Journal of Engineering, Vol. 18, pp. 340–348, Mar. 2012.
[8] Marro G., Prattichizzo D., and Zattoni E., "*Geometric Insight into Discrete-time Cheap and Singular Linear Quadratic Riccati (LQR) Problems*", IEEE Transactions on Automatic Control, Vol. 47, No. 1, pp. 102–107, 2002.
[9] Ang H. K., Chong G., and Li Y., "*PID Control System Analysis, Design, and Technology*", IEEE Transactions on Control System Technology, Vol. 13, pp. 559–576, 2005.
[10] Yaniv O. and Nagurka M., "*Robust, PI Controller Design Satisfying Sensitivity and Uncertainty Specifications*", IEEE Transactions on Automation Control, Vol. 48, pp. 2069–2072, 2003.
[11] Meshram P. M. and Kanojiya R. G., "*Tuning of PID Controller using Ziegler-Nichols Method for Speed Control of DC Motor*", IEEE International Conference On Advances In Engineering, Science and Management (ICAESM-2012), pp. 117–122, Mar. 2012.
[12] Praboo N. N. and Bhaba P. K., "*Simulation work on Fractional Order PI Control Strategy for Control of DC Motor based on Stability boundary Locus Method*", International Journal of Engineering Trends and Technology, Vol. 4, Issue 8, pp. 3403–3409, 2013.
[13] Alasooly H., "*Control of DC Motor using Different Controller Strategies*", Global Journal of Technology and Optimization, Vol. 2, pp. 21–28, 2011.